Revue des Composites et des Matériaux Avancés-Journal of Composite and Advanced Materials
Vol. 35, No. 3, June, 2025, pp. 497-505
Journal homepage: http://iieta.org/journals/rcma

Characterization of Y_2O_3 and/or SiC Reinforced Al on Tribological Behaviour

Manar Assaf Al-Kinani*, Saad Hameed Al-Shafaie

Department of Metallurgical Engineering, College of Materials Engineering, University of Babylon, Hilla 51001, Iraq

Corresponding Author Email: mat.manar.assaf@uobabylon.edu.iq

https://doi.org/10.18280/rcma.350311

Received: 1 April 2025
Revised: 3 May 2025
Accepted: 18 May 2025
Available online: 30 June 2025

Keywords:
HAMMCs, Al alloys, Y_2O_3, SiC, stir casting, wear rate

ABSTRACT

This study acknowledges the use of ceramics, such as SiC and/or Y2O3, in the stir casting technique for the producing AMMCs. Hardness, coefficient of friction and wear behavior of the prepared MMCs were evaluated. The results of the testing showed that the unreinforced matrix was not as hard as the reinforced matrix (16%). Wear resistance raised steadily due to the SiC and Y_2O_3 particle loading, both alone and in combination. Using Optical and scanning electron microscopes (SEM) to examine the microstructure and worn surface, it was discovered that mechanically mixed layers of SiC and Y_2O_3 had formed. These layers acted as an effective insulating surface, preventing the test sample surface from contacting the zirconia pins. weight loss decreased when the reinforcing materials were changed, and at 5% SiC, notable wear resistance was attained.

1. INTRODUCTION

A composite material is formed by combining a matrix with a reinforcing component, when combined, has better qualities than either material alone. A composite material composed of at least two components, one of which can be either metal or mostly ceramic, is called a metal matrix composite [1]. MMCs have been evaluated as viable options to satisfy this service demand desire. This is due to their remarkable qualities, that involve a favorable mix of surface and mechanical properties, suitability for tried-and-true conventional operating methods, and low processing costs [2, 3]. The cost of fabricating Discontinuously reinforced MMCs is significantly lower than that of continuously reinforced composites. Therefore, compared to aligned reinforcements discontinuous reinforcements result in lower incremental expenditure for improving matrix performance. Compared to reinforced composites, particulate-reinforced MMCs are less costly to produce. Therefore, compared to fiber-aligned reinforcements increases matrix performance at a lower cost. Furthermore, particle-reinforced composites have isotropic characteristics [4]. Although, composites with fiber-oriented reinforcements have extremely non-isotropic characteristics [5]. The improved hardness, creep resistance, and specific strength characteristics of hybrid MMCs make them a great alternative to traditional materials [6].

In addition to aerospace applications like the wing and fuselage (primary body) of aircraft structures, internal aerospace engine components, and exhaust systems, HAMMC discovered several significant engineering uses, including cylinder liners, bearing surfaces, brake parts, camshafts, and pistons [7]. The most often utilized forms of reinforcement in HAMMCs are Al_2O_3, Si_3N_4, SiC, Y_2O_3, and TiC [8, 9]. The most popular forms of reinforcement that are available for usage attributed to their hardness, high strength, thermal conductivity, and melting point, Y_2O_3 and SiC were chosen as the reinforcement to be employed in this investigation [10-12]. It is useful for these ceramics were chosen as the study's reinforcement because the hard particles SiC and Y_2O_3 are used in this study to strengthen the aluminium composite. The strengthening is warranted given that SiC and Y_2O_3 are promising candidates to investigate enhanced tribological and mechanical properties [13]. Liquid methods are frequently used to treat aluminum composites [14, 15]. The liquid method of casting is called “route casting”, and in this process, a stirring machine that is mechanical is used to create a swirling motion that combines the matrix with reinforcement. Because of its affordability, validity of mass production, ease of use, nearly net shaping, and simpler control over metal matrix composite may be effectively created using the composite structure [16]. Zhang and Li [17] employed alumina and graphene to enhance the lubricating characteristics of hybrid MMCs. The primary reason for using graphene as reinforcement in hybrid composites is due to its self-lubricating substance. When Al_2O_3 is used as reinforcement, it will make the composite stronger than the master alloy (MA). Subramaniam et al. [18] described the production and evaluation of mechanical properties of Aluminium 7075 reinforced with fly ash particles from coconut shell and boron carbide (B_4C) and produced with using stir casting process. (0, 3, 6, 9, and 12 wt percent of B_4C) and (3 wt percent) of fly ash were used to create the Al7075 HAMC specimens. These results show that while ductility reduces with more reinforcing particles with the matrix, hybrid composites' mechanical characteristics, like tensile strength and hardness, improve. Comparing maximum tensile strength to unreinforced

aluminum 7075, it increased by 66%. Several reinforcements promote interface bonding and decrease porosity. AM et al. [19] both age hardening and non-age hardening wear tests were carried out at ambient temperature under certain circumstances. SiC and Al_2O_3 are the reinforcement materials, and Al7075 has been selected as the matrix. It is obvious from the data that the HAMMCs exceed the unreinforced aluminum alloy in terms of tribological characteristics. Hlail and Al-Shafaie [7] were used the optimization especially Grey Relational Analysis (GRA) to enhance the mechanical characteristics of Al reinforced single and multi of SiC and Al_2O_3. For the manufactured MMCs, measurements have been made of their mechanical characteristics, including yield strength, hardness, elongation, tensile strength, and flexural strength. The research Results indicate that every reinforcing material significantly affects response, the hybrid MMCs' response qualities were enhanced by the Taguchi-based GRA technique.

Cui et al. [20] carried out a sintered by powder metallurgy process to prepare Co- $MoSi_2$ composite so as to avoid the component failure induced by high-temperature wear damage. In particular, compared with MA, the Co matrix composites exhibited superior tribological behavior for the temperature ranges 25-1000℃ owing to the high wettability of $MoSi_2$, mechanical properties and oxide lubricating film. Nahi et al. [1] added B_4C and/or SiC particles using GRA to enhance the mechanical characteristics of Al7075 alloy. yield strength, hardness, elongation, tensile strength, and flexural strength were among the mechanical characteristics of AMMCs that were examined. Comparing the mechanical characteristics to the MA, outcomes showed increased mechanical characteristics. The best factor combination was shown in the experiment, and the expected and actual values were more alike. Thakur et al. [21] utilized stir casting to fabricate the Al6063 alloy, employing B_4C and/or Gr as the reinforcing agents. SEM indicating the isotropic reinforcement in different composite casts, energy dispersive X-ray diffraction, and XRD graphs have all been accustomed to study the samples' morphology. According to the wear test, for a given weight and sliding speed composites overall surface morphology much improved. The wear rate was recorded at its greatest for pure-Al and at its minimum for Al-B_4C-Gr 5% with friction coefficient differing between the two. The addition of Gr to the hybrid composite improves both wear resistance and the amount of friction between the sliding sides. The pure-Al pin exhibits the maximum surface degradation in terms of groove creation, delamination, as well as abrasion, whereas the Al-B_4C composite shows less delamination and grooves, according to SEM images. The Gr protective tribological coating that forms in the hybrid MMC, Al-B_4C-Gr (2 - 5)%, results in smooth tracks and minimum delamination and fracture propagation.

According to the discussion above, there is a lack of information concerning the behaviour of composites under dry sliding wear conditions reinforced with one or more ceramics. This research focuses on determining how the wear properties of Al-Y_2O_3 and/or SiC MMCs are affected. Response surface methodology was engaged to identify wear properties of the MA and the composites, in order to increase the accuracy of the evaluation. To examine its behavior, the test samples underwent wear, density, porosity, and hardness testing. The microstructure and phase analysis were assessed using SEM and XRD methods, accordingly. The RSM method's applicability in forecasting the importance of experimental outcomes and determining the key elements influencing the wear properties of composites was investigated.

2. EXPERIMENTAL DETAILS

2.1 Fabrication of MA and MMC

The MA utilized in this work, Al-3.0% Mg, was made by the stir casting route, in which mg has been added to pure aluminum wires for the purpose of improving the wettability of reinforcement particles by reducing their surface tension. The molten MA was poured into a die casting mold that is 20 mm in diameter and 100 mm in height. Table 1 displays the composition of the MA.

Yttria and/or Silicon Carbide with an average size of the particle (5.323 μm and 22.510 μm) separately in the order were used as reinforcement, as shown in Figure 1. The composites shown in Table 2 were made using the vortex technique. After mixing the quantity of Al base into the graphite crucible, the temperature was elevated to 750℃ and maintained until the MA had melted completely. The reinforcement particles (Y_2O_3, SiC, and Y_2O_3 + SiC) with (5% wt) of strengthening particles were unique and simultaneously were covered with foil made of Al, heated to 300℃, followed by being added gradually to the liquid metal. After stirring for five minutes at 450℃, the strengthening particles were equally distributed in the molten MA.

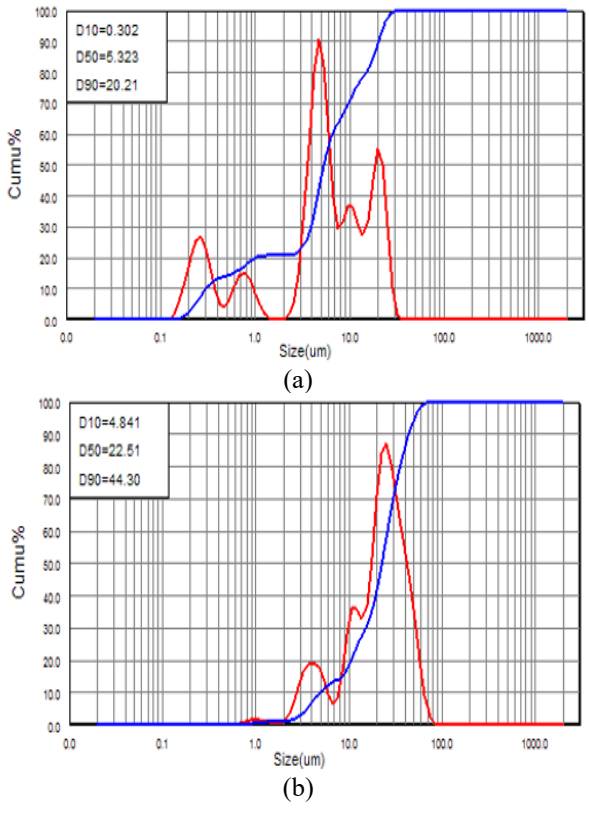

Figure 1. The particle size distribution for (a) Y_2O_3 and (b) SiC

2.2 Microstructure observation

A sample of the MA and Al- Y_2O_3 and/or SiC was collected and cold-mounted using polyester resin that cures at room temperature. The standard metallographic method was

followed. Up to 2000, gradually finer grades of emery papers underwent Rough polishing using a diamond paste with a particle size of 5µm. After being carefully cleaned with distilled water and dried in an air blast, the samples were kept in a desiccator for as little time as possible before etching. A chemical etchant (Keller Etch) was used to etch the polished samples. Then investigated using an optical microscope (OM) at a magnification of 60X.

2.3 X-ray diffraction analysis

The phases in the alloys were identified using XRD methods to study each specimen individually. The X-ray machine utilized was a SHIMADZU XRD-6000 Lab X, Japan. The X-ray generator with a filter from Ni and Cu Kα radiation i.e., (λ = 1.5406 ºA). The diffraction angle 2θº ranged from 20º to 80º, and the diffractometer scanning speed was set at 5 degrees per minute.

Table 1. MA's composition

Element	Si	Mn	Fe	Mg	Cu	Zn	Al
%Weight	0.0801	0.0832	0.203	3.0	0.014	0.0047	Rem.

Table 2. Mass fraction of materials

Sample Designations	Material Mixing Ratio (%)		
	Al	Y_2O_3	SiC
S	100	0	0
S1	95	5	0
S2	95	0	5
S3	95	2.5	2.5

Table 3. Conditions of the dry sliding wear test

Parameters	Value
Applied Load	10, 15 and 20N
Sliding Speed	6.2831, 7.8539, and 9.4247 m/min
Test Duration	30 min

2.4 Tribological test

As seen in Figures 2 and 3, tribological tests were carried out at room temperature in a tribotester of the pin-on-disc kind (MT-4003, version 10). The pin (ZrO_2), having a 10 mm diameter wear track, is kept against the counterface of a rotating disk. The loading lever applies loads to the pin while the disk provides sliding speeds. The coefficient of friction (CoF), which is shown on the monitor, is measured by a sensor that is connected to the lever. By utilizing a pin-on-disk tribometer to change the reinforced materials (Y_2O_3 and/or SiC) and altering the load and speed for approximately half an hour, the weight loss of the test sample was determined by subtracting the sample weight both prior to and following the test using a pin-on-disc tribometer. The response Surface Methodology's test conditions were followed for conducting the experiments [22-24]. Table 3 displays the specific design parameters and their levels for the tribological testing. To ensure contact between the zirconia pin and the flat surfaces, the specimens were polished, making use of emery paper (1000-size grit) prior to the wear testing. The sample and wear track are cleaned with acetone.

Figure 2. Wear (pin-on-disk) and friction tribotester

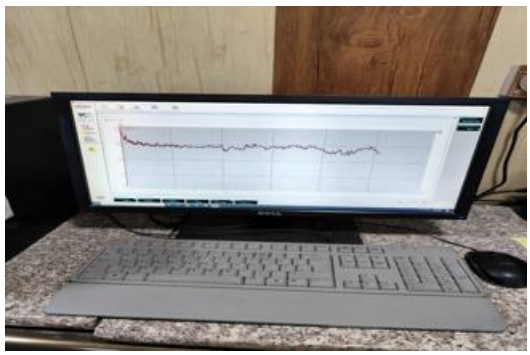

Figure 3. Friction and wear monitor connected to tribotester

3. RESULTS AND DISCUSSION

3.1. XRD analysis and study of microstructural

An optical micrograph of MA and Al-Y_2O_3 and/or SiC MMCs at different reinforcing levels is displayed in Figure 4(a). The microstructure indicated that the reinforcing particles were distributed uniformly throughout the base material Al alloy. This was attributed to the effectiveness of the vortex movement as well as the adoption of an appropriate composite production technique. The reinforcement particles were found to cluster in all samples (S1-S3) since each composite had the same number of reinforcements. Clustering is influenced by Size, quantity, and stirring time during the stir casting process. Four samples are made up of five percent each of Y_2O_3, SiC alone, and hybrid (Y_2O_3 and SiC together). Due to the same amount of reinforcement is applied throughout the sample, the clustering is essentially equal.

Al's existence was verified by the XRD analysis, which

showed a higher peak. Minimum peaks at all samples test pins clearly showed the presence of Y_2O_3 and SiC, either separately or in combination. The XRD spectrum revealed that Cu was present in every test pin as a common component, as seen in Figure 4(b). Figure 4(b) shows the specifics of the X-ray diffraction study for the constituents present. X-ray patterns were obtained by transmitting the X-ray Cu-K radiation through the materials. Sample S showed the largest peak for aluminum, as shown in Figure 3. Alternatively, Cu showed additional peaks. The three strongest peaks for aluminium, Gr, and B_4C were easily visible from specimen S2. While Cu, B_4C, and Gr in S3 and S4 showed many peaks, the most significant peak for aluminium was clearly visible. Different strengthenings, such as aluminium B_4C and Gr, were found after comparing the experimental peaks with ordinary peaks. X-ray diffraction revealed the presence of B_4C and Gr.

3.2 Hardness test

Figure 5 describes both the MA and the filler-enhanced alloy's hardness. It has been noted that all manufactured composites have a comparatively higher hardness than MA. According to measurements, the Al/Y_2O_3 composite's mean hardness is 80 HV, which is 7.5% more than the MA's. The SiC fills register the highest rise of 16%. The highest hardness value recorded among all manufactured composite is 88 HV, which is the mean hardness of the Al/ SiC composite. A 10% improvement in mean hardness, from 74 HV to 82 HV, has been achieved in the reinforcement of hybrid fillers, which includes Y_2O_3 and SiC particles. It has been noted that the filler strengthening improves the studied property of MMCs.

3.3 Frictional and wear behavior

A tribotester of the pin-on-disc type is employed to estimate the friction and wear properties of the MA, Al-Y_2O_3, and/or SiC MMCs reinforced with 5% of second phase particles by adjusting the sliding speed and normal load. For thirty minutes, the duration of the slidings remains unchanged. In this part, microstructural characterization is examined together with the impact of sliding speed and imposed load on the tribological characteristics.

3.3.1 Frictional behavior

Figure 6 illustrates how the CoF of MA, Al-Y_2O_3, and/or SiC MMCs changes with applied normal load. The figure shows that the CoF generally falls for all alloys as applied normal load increases. Typically, when the pin slips on MA or S, it displays a high CoF. This is MA's main flow, which may be fixed by altering it by adding SiC and Y_2O_3 either independently or combined. Al-Y_2O_3 and/or SiC MMCs display a decrease in CoF as the applied load increases in comparison to MA. According to Natarajan et al., this could occur as a result of a transfer layer forming at the contacting surface [25]. The figure illustrates the effect of rising hardness on reduction of CoF, as the result of comparing four alloy MMCs. It seems natural that friction will decrease as the hardness increases. CoF varies with sliding speed for different applied normal loads, as seen in Figure 7. With the change in loads, the CoF exhibits the same behavior as previously explained, according to the schematic, and for the same reasons.

3.3.2 Wear behavior

Figure 8 shows how wear (weight loss) changes with applied stress for MA, Al-Y_2O_3, and/or SiC MMCs under different sliding speeds. According to the figure, weight loss increases as applied stress improves. According to Pradhan et al., the large applied normal load causes shear, which causes fracture of reinforcing particles in the matrix composite. Progressively, MMC wear is due to this degradation of the metal matrix's mechanical properties [26]. Consequently, it might be claimed that wear becomes better as the applied stress increases. Wear changes with sliding distance, as seen in Figure 9. Wear becomes better as the sliding distance increases. Additionally, when hardness increases, it often decreases in response to variation in applied load. The MMCs with high hardness showed very little wear loss. Bauri and Surappa [27] have demonstrated that adding Y_2O_3 and/or SiC particles increases resistance to wear.

3.3.3 Worn surface morphology

According to the SEM images of the MA, Al-Y_2O_3, and/or SiC MMCs alloy shown in Figure 10, the worn abraded surface was parallel to the sliding direction. The abraded surface of the MA alloy (Figure 10(a)) showed significant material flow and distortion, demonstrating the adhesive wear process. Figure 10(b) illustrates how detached wear debris caused scratches and cutting, also known as micro-ploughing, which resulted in deeper grooves in the sliding direction and re-melted bubbles. In Figure 10(c), the surface tribo-layer, suggested as the protective layer, showed a reduction in weight loss. Figure 10(d) reveals the microstructure of the Al-Y2O3/SiC composite, where the combination of Al-Y_2O_3 and SiC particles contributes to the enhanced wear resistance and reduced deformation compared to the individual components. The wear behavior was also affected by the Al-SiC interfacial strength. As seen in Figure 10, a stronger interfacial may lead to improved wear resistance.

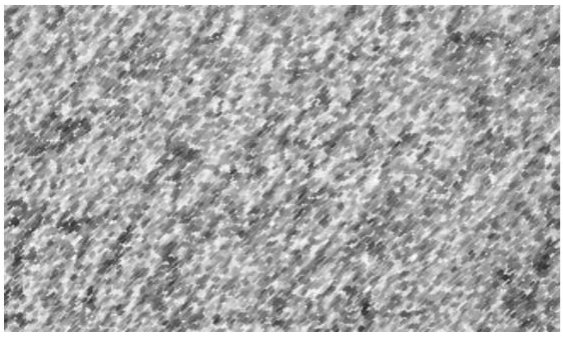

S

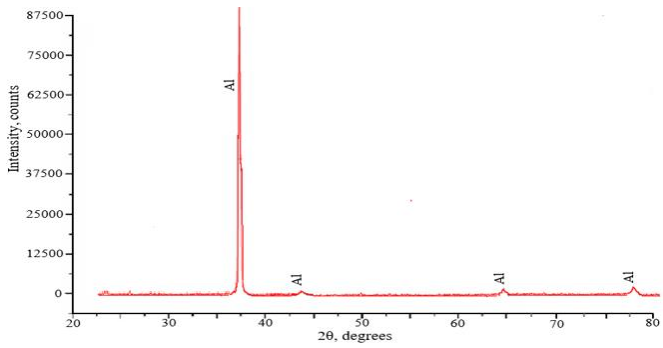

S

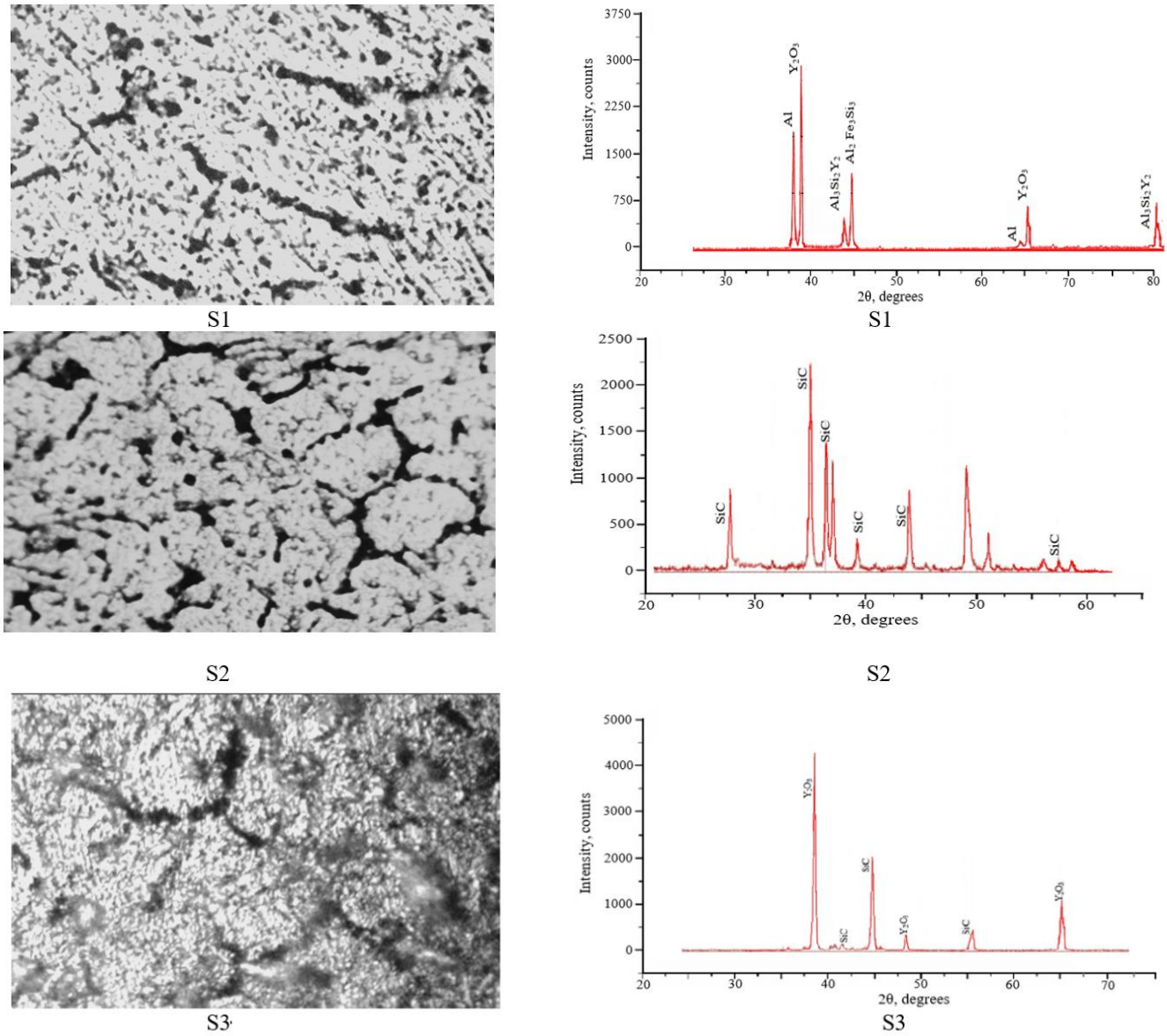

Figure 4. (a) Optical photomicrographs and (b) XRD of S, S1, S2, and S3

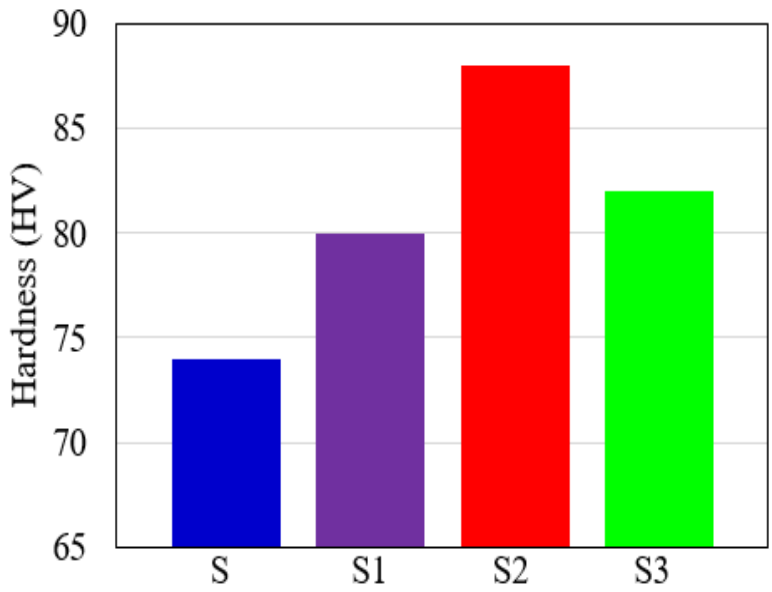

Figure 5. Hardness value of the sample

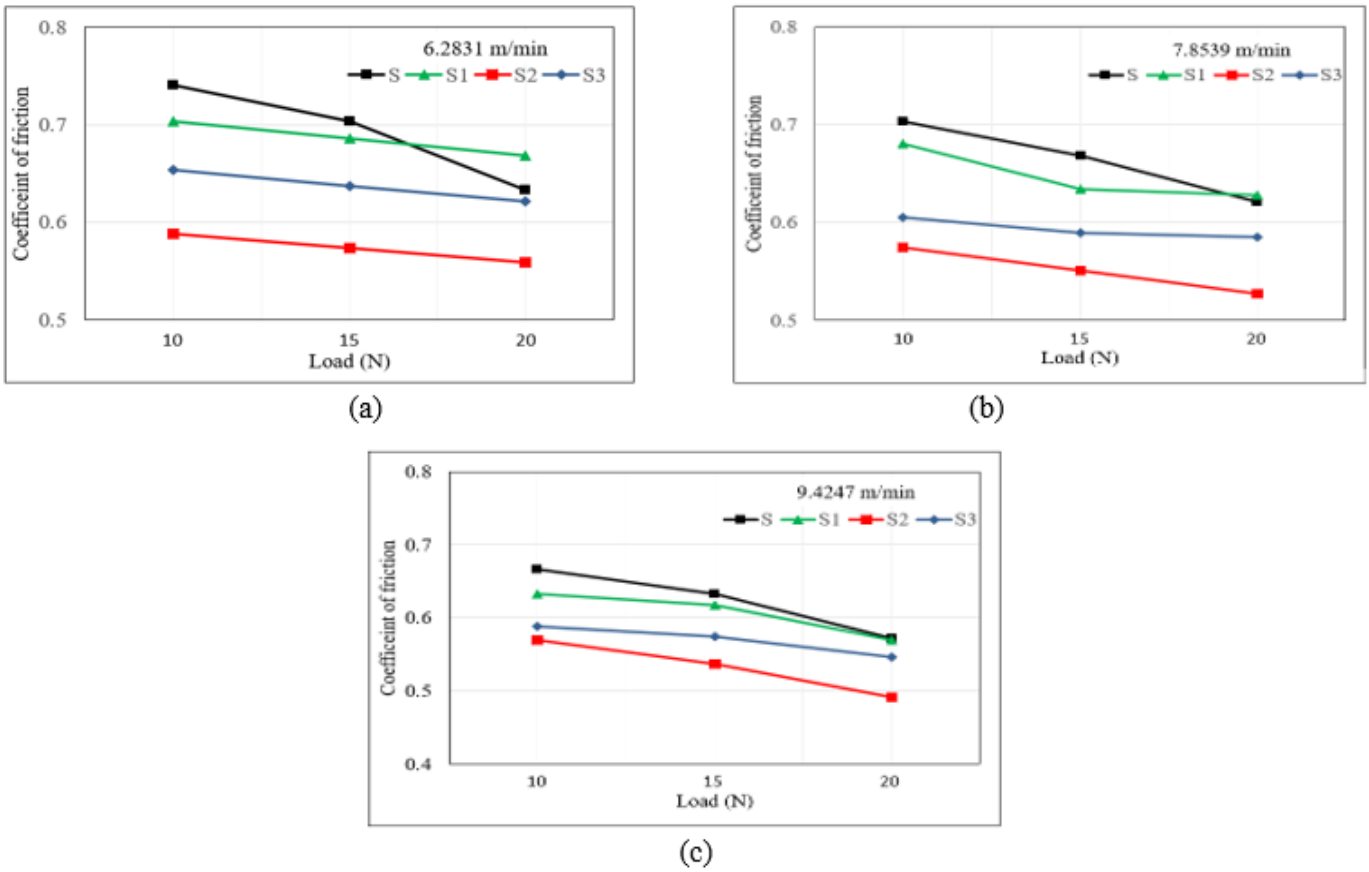

Figure 6. CoF vs. applied load for different sliding speed: (a) 6.2831 m/min, (b) 7.8539 m/min and (c) 9.4247 m/min

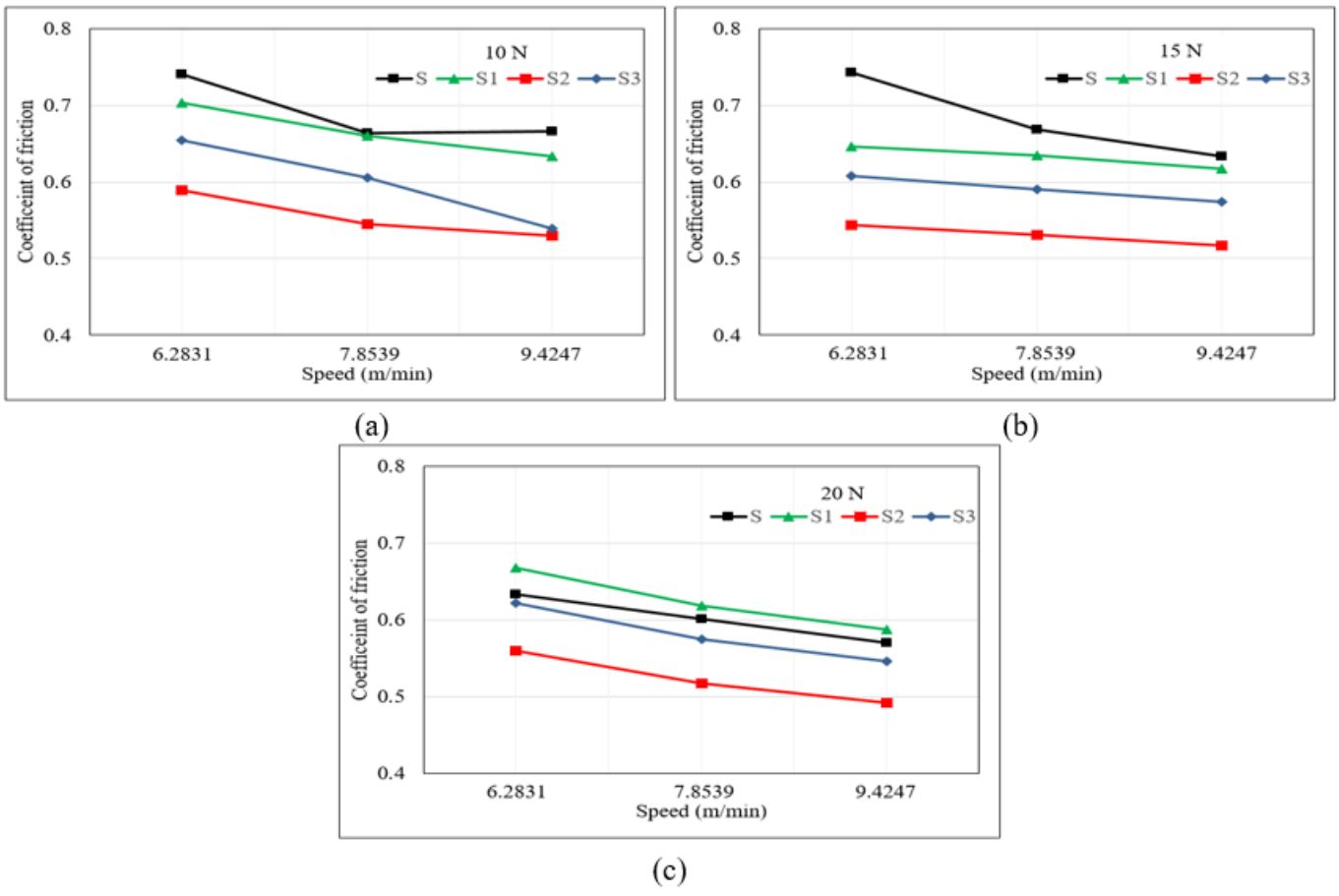

Figure 7. CoF vs. sliding speed under varying normal load: (a) 10 N, (b) 15 N and (c) 20 N

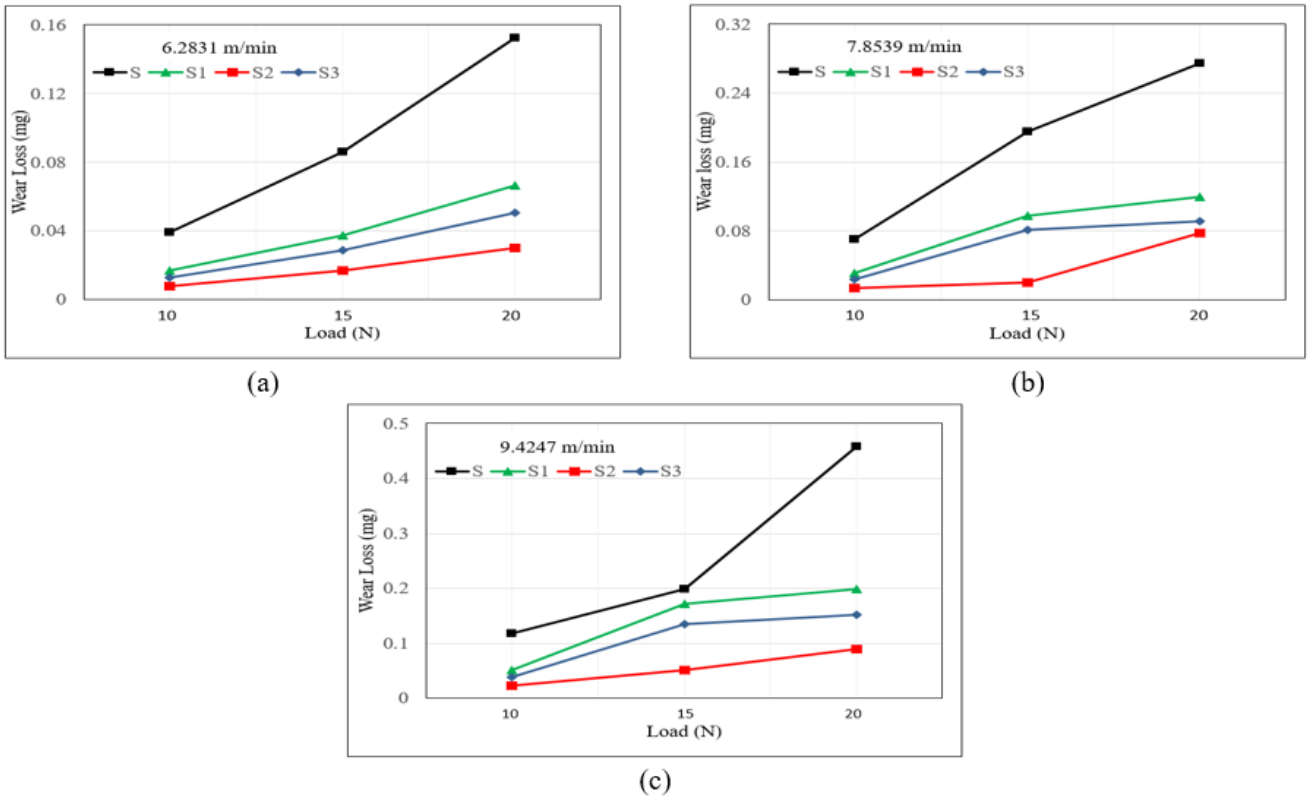

Figure 8. wear vs. applied load for different sliding speed: (a) 6.2831 m/min, (b) 7.8539 m/min and (c) 9.4247 m/min

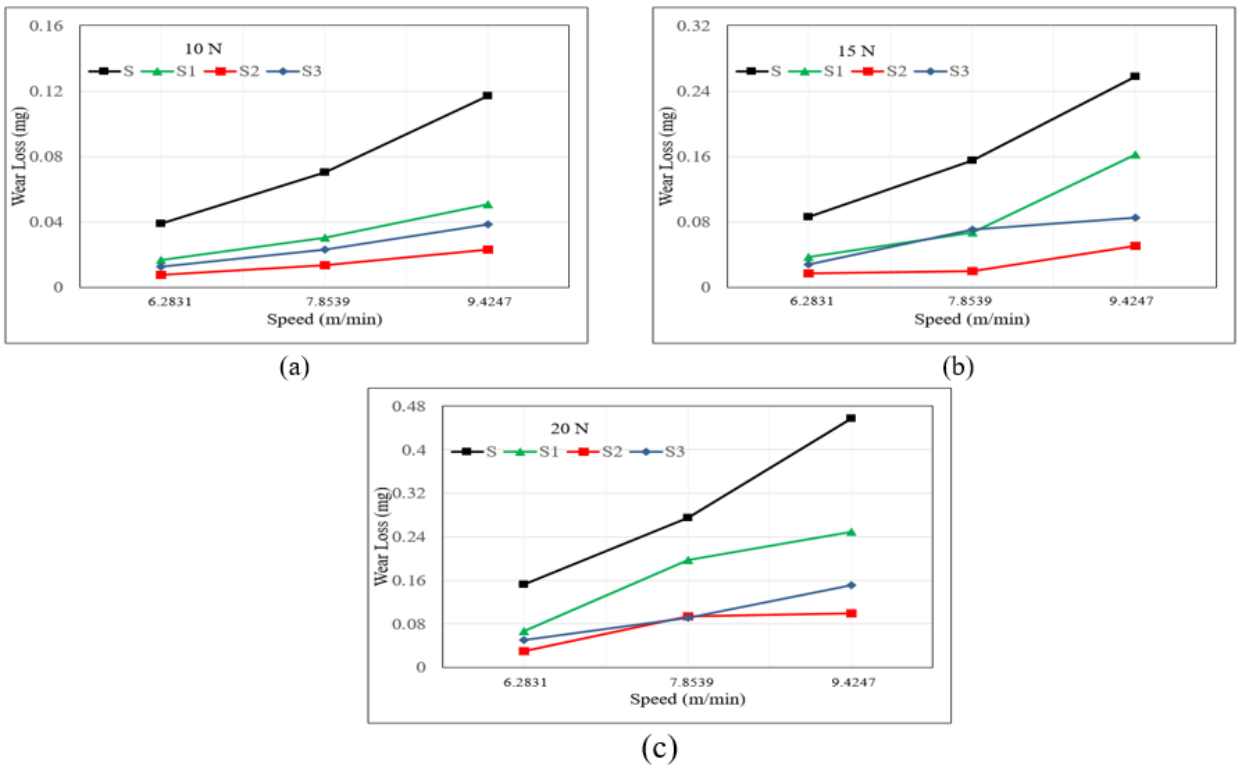

Figure 9. Wear vs. sliding speed for different load: (a) 10 N, (b) 15 N, and (c) 20 N

3.3.3 Worn surface morphology

According to the SEM images of the MA, Al-Y_2O_3, and/or SiC MMCs alloy shown in Figure 10, the worn abraded surface was parallel to the sliding direction. The abraded surface of the MA alloy (Figure 10(a)) showed significant material flow and distortion, demonstrating the adhesive wear process. Figure 10(b) illustrates how detached wear debris caused scratches and cutting, also known as micro-ploughing, which resulted in deeper grooves in the sliding direction and re-melted bubbles. In Figure 10(c), the surface tribo-layer, suggested as the protective layer, showed a reduction in weight loss. Figure 10(d) reveals the microstructure of the Al-Y2O3/SiC composite, where the combination of Al-Y_2O_3 and

SiC particles contributes to the enhanced wear resistance and reduced deformation compared to the individual components. The wear behavior was also affected by the Al-SiC interfacial strength. As seen in Figure 10, a stronger interfacial may lead to improved wear resistance.

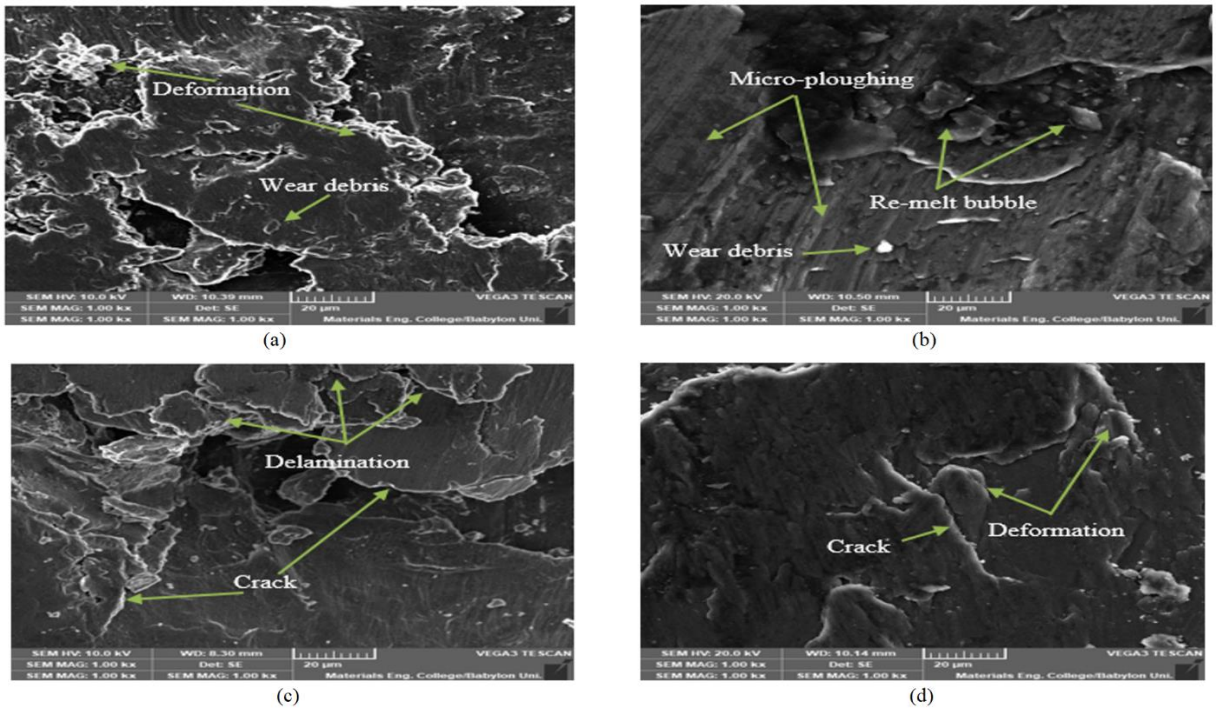

Figure 10. Microstructure of abraded disk at 20 N applied load in addition to 9.4247 m/min sliding speed: (a) MA, (b) Al/Y_2O_3, (c) Al/SiC and (d) Al/Y_2O_3/ SiC

4. CONCLUSIONS

1. The SiC reinforced matrix was the hardest alloy (16%) of the base alloy.
2. Optical microstructure of the MMCs revealed that the matrix material's distribution of the reinforcement is uniform.
3. Hardness was raised by adding Y_2O_3 and/or SiC particles over the matrix, acting as a dislocation barrier.
4. Hardness was directly correlated with wear resistance and inversely with coefficient of friction.
5. The weight reduction for the 5 wt. % SiC was substantially smaller.

5. SUGGESTION FOR FUTURE WORK

1. A different method like rheo casting friction stir process could be utilized for sample fabrication.
2. Nano size particles could also be use, as this may facilitate the dispersion of reinforcing particles at the nanoscale.
3. Certain conditions like wet wear and temperature of pin and disk were look to be a significant. This could be also believed to be a determinant in some future work.
4. Grey Relational Analysis and Genetic Algorithm analysis could also be done in future work to improve a more exact statistical modeling and optimization.

REFERENCES

[1] Nahi, M.S., Al-Shafaie, S.H., Jasim, S.A. (2023). Improving the mechanical properties of Al7075 alloy by adding B4C and/or SiC particles using gray relational analysis. In AIP Conference Proceedings, 2830(1): 030030. https://doi.org/10.1063/5.0157529

[2] Alaneme, K.K., Bodunrin, M.O., Awe, A.A. (2018). Microstructure, mechanical and fracture properties of groundnut shell ash and silicon carbide dispersion strengthened aluminium matrix composites. Journal of King Saud University-Engineering Sciences, 30(1): 96-103. https://doi.org/10.1016/j.jksues.2016.01.001

[3] Alaneme, K.K., Ajibuwa, O.A., Kolawole, I.E., Fajemisin, A.V. (2017). Mechanical, corrosion and wear behaviour of steel chips and graphite reinforced Zn-27Al alloy based composites. Acta Metallurgica Slovaca, 23(2): 171-181. https://doi.org/10.12776/ ams.v23i2.865

[4] Mahdi, F.M., Annaz, A.U.A. (2015). Effect of Yttria content up to 15 wt% on mechanical properties of Al-Y2O3 composites prepared via squeeze casting and powder metallurgy routes. Sulaimani Journal for Engineering Sciences, 2: 55-64. https://doi.org/10.17656/sjes.10024

[5] Lewis, C., Yavuz, B.O., Longana, M.L., Belnoue, J.P.H., Ramakrishnan, K.R., Ward, C., Hamerton, I. (2024). A Review on the Modelling of Aligned Discontinuous Fibre Composites. Journal of Composites Science, 8(8): 318. https://doi.org/10.3390/jcs8080318

[6] Rajesh, A.M., Kaleemulla, M.K., Doddamani, S. (2019). Effect of Heat Treatment on Wear behavior of Hybrid Aluminum Metal Matrix Composites. Tribology in Industry, 41(3): 344. https://doi.org/10.24874/ti.2019.41.03.04

[7] Hlail, H.H., Al-Shafaie, S.H. (2020). Multi-response

optimization of mechanical properties of Al reinforced by Al2O3 and/or SiC using grey relational analysis. IOP Conference Series: Materials Science and Engineering, 671(1): 012012. https://doi.org/10.1088/1757-899X/671/1/012012

[8] Karantzalis, A.E., Wyatt, S., Kennedy, A.R. (1997). The mechanical properties of Al-TiC metal matrix composites fabricated by a flux-casting technique. Materials Science and Engineering: A, 237(2): 200-206. https://doi.org/10.1016/S0921-5093(97)00290-6

[9] Hossein-Zadeh, M., Razavi, M., Mirzaee, O., Ghaderi, R. (2013). Characterization of properties of Al–Al2O3 nano-composite synthesized via milling and subsequent casting. Journal of King Saud University-Engineering Sciences, 25(1): 75-80. https://doi.org/10.1016/j.jksues.2012.03.001

[10] Ianoş, R., Băbuţă, R., Lazău, R. (2014). Characteristics of Y2O3 powders prepared by solution combustion synthesis in the light of a new thermodynamic approach. Ceramics International, 40(8): 12207-12211. https://doi.org/10.1016/j.ceramint.2014.04.062

[11] Chaim, R., Shlayer, A., Estournes, C. (2009). Densification of nanocrystalline Y2O3 ceramic powder by spark plasma sintering. Journal of the European Ceramic Society, 29(1): 91-98. https://doi.org/10.1016/j.jeurceramsoc.2008.05.043

[12] Nahi, M.S., Al-Shafaie, S.H., Jasim, S.A. (2023). Multi-objective optimization in electrical discharge machining of SiC and/or B4C reinforced Al7075 using grey relational analysis. In AIP Conference Proceedings 2830(1): 030021. AIP conference proceedings. https://doi.org/10.1063/5.0157310

[13] Natarajan, P., Sekar, T., Chenrayan, V., Rajeshkumar, L. (2025). The effect of SiC and Y2O3 inclusion on microstructure and mechanical properties of Al 5052 composite fabricated through Friction Stir Process. Heliyon, 11(1): e41665. https://doi.org/10.1016/j.heliyon.2025.e41665

[14] Georgantzia, E., Gkantou, M., Kamaris, G.S. (2021). Aluminium alloys as structural material: A review of research. Engineering Structures, 227: 111372. https://doi.org/10.1016/j.engstruct.2020.111372

[15] Zhu, J., Jiang, W., Li, G., Guan, F., Yu, Y., Fan, Z. (2020). Microstructure and mechanical properties of SiCnp/Al6082 aluminum matrix composites prepared by squeeze casting combined with stir casting. Journal of Materials Processing Technology, 283: 116699. https://doi.org/10.1016/j.jmatprotec.2020.116699

[16] Ramnath, B.V., Elanchezhian, C., Jaivignesh, M., Rajesh, S., Parswajinan, C., Ghias, A.S.A. (2014). Evaluation of mechanical properties of aluminium alloy–alumina–boron carbide metal matrix composites. Materials & Design, 58: 332-338. https://doi.org/10.1016/j.matdes.2014.01.068

[17] Zhang, Y., Li, X. (2017). Bioinspired, graphene/Al2O3 doubly reinforced aluminum composites with high strength and toughness. Nano Letters, 17(11): 6907-6915. https://doi.org/10.1021/acs.nanolett.7b03308

[18] Subramaniam, B., Natarajan, B., Kaliyaperumal, B., Chelladurai, S.J.S. (2018). Investigation on mechanical properties of aluminium 7075-boron carbide-coconut shell fly ash reinforced hybrid metal matrix composites. China Foundry, 15: 449-456. https://doi.org/10.1007/s41230-018-8105-3

[19] AM, R., Kaleemulla, M., Doddamani, S., KN, B. (2019). Material characterization of SiC and Al2O3–reinforced hybrid aluminum metal matrix composites on wear behavior. Advanced Composites Letters, 28: 0963693519856356. https://doi.org/10.1177/0963693519856356

[20] Cui, G., You, S., Li, F., Niu, M., Gao, G., Liu, Y. (2023). High-temperature wear and friction behavior of Co matrix composites reinforced by MoSi2 over a wide temperature range. Tribology International, 189: 108920. https://doi.org/10.1016/j.triboint.2023.108920

[21] Thakur, A., Murtaza, Q., Ahmed, J., Choon Kit, C., Prakash, C., Khanna, V., Liu, L.W. (2024). Evaluation of tribological parameters for boron carbide and graphite infused aluminium hybrid composite fabricated by stir casting technique. Scientific Reports, 14(1): 23303. https://doi.org/10.1038/s41598-024-73877-9

[22] Al-Kinani, M.A. (2023). Optimizing tensile strength and hardness in FSW of AA 6061 and AA 7075 via RSM and desirability function. Annales de Chimie - Science des Matériaux, 47(6): 411-416. https://doi.org/10.18280/acsm.470608

[23] Mahdy, H.F., Al-Kinani, M.A., Al-Shafaie, S.H., Jailawi, R.M. (2021). Mathematical modeling for performance measure on the electrical discharge machining of inconel 718 by response surface methodology. Journal of Mechanical Engineering Research and Developments, 44: 363-374.

[24] Al-Mousawi, M.A., Al-Shafaie, S.H., Khulief, Z.T. (2024). Modeling and analysis of process parameters in EDM of Ni35Ti35Zr15Cu10Sn5 high-temperature high entropy shape memory alloy by RSM Approach. Manufacturing Review, 11: 4. https://doi.org/10.1051/mfreview/2024002

[25] Natarajan, N., Vijayarangan, S., Rajendran, I. (2006). Wear behaviour of A356/25SiCp aluminium matrix composites sliding against automobile friction material. Wear, 261(7): 812-822. https://doi.org/10.1016/j.wear.2006.01.011

[26] Pradhan, S., Ghosh, S., Barman, T.K., Sahoo, P. (2017). Tribological behavior of Al-SiC metal matrix composite under dry, aqueous and alkaline medium. Silicon, 9: 923-931. https://doi.org/10.1007/s12633-016-9504-y

[27] Bauri, R., Surappa, M.K. (2008). Sliding wear behavior of Al–Li–SiCp composites. Wear, 265: 11-12, 1756-1766. https://doi.org/10.1016/j.wear.2008.04.022